Insert Title: Focused Ultrasound Modulation of BOLD Functional Connectivity

First A. Author, *Member, IEEE*, Second B. Author, and Third C. Author

Abstract

This paragraph summarizes the motivation for investigating focused ultrasound neuromodulation, the experimental design, and the main outcomes on BOLD functional connectivity. Mention the primary hypothesis, key quantitative findings, and relevance to translational neuroengineering.

Index Terms

Focused ultrasound, BOLD fMRI, functional connectivity, neuromodulation, biomedical engineering

I. Introduction

Introduce the scientific motivation, prior work on low-intensity focused ultrasound (FUS) neuromodulation, and the translational significance for neuropsychiatric disorders. Clearly state the open question this manuscript addresses and outline the contributions:

- Quantify baseline resting-state connectivity patterns in the sgACC and distributed networks.
- Model acute changes in functional connectivity induced by FUS stimulation.
- Provide mechanistic interpretation that links FUS dose, targeting accuracy, and network-level responses.

Conclude with a roadmap of the paper.

II. Materials and Methods

Describe participant selection, ethics approvals, imaging protocols, preprocessing, and statistical analyses. Structure the section with descriptive subheadings such as:

A. Participants and Study Design

Summarize demographics, inclusion/exclusion criteria, and experimental timeline. Reference relevant IRB approvals and informed consent procedures.

Manuscript received Month DD, YYYY; revised Month DD, YYYY; accepted Month DD, YYYY. Date of publication Month DD, YYYY; date of current version Month DD, YYYY. This work was supported by XYZ (grant number). (Corresponding author: First Author.)

First Author and Second Author are with the Department of Biomedical Engineering, Example University, City, State ZIP, USA (e-mail: first.author@example.edu).

Third Author is with the Department of Neurology, Example Medical Center, City, State ZIP, USA.

Color versions of one or more of the figures in this article are available online at https://ieeexplore.ieee.org.

Digital Object Identifier (DOI): 10.1109/TBME.XXXX.XXXXXXX

B. Focused Ultrasound Targeting

Provide acoustic parameters (frequency, pulse repetition, duty cycle, intensity) and targeting workflow (e.g., neuronavigation, safety monitoring).

C. MRI Acquisition

Detail scanner hardware, BOLD sequence parameters, structural scans, and physiological monitoring.

D. Preprocessing and Quality Control

Outline motion correction, susceptibility distortion correction, spatial normalization, temporal filtering, and frame censoring thresholds.

E. Functional Connectivity Analysis

Mixed-effects analysis of sgACC connectivity: To formally test whether transcranial focused ultrasound (tFUS) altered the temporal evolution of subgenual ACC (sgACC) connectivity beyond sham, we analyzed sgACC-centered functional connectivity (FC) at the *subject level*, avoiding edge-wise pseudoreplication. For each subject, condition (active, sham), and time window (pre: 60–300 s, fus: 300–600 s, post: 600–900 s), we computed the mean FC between the sgACC DiFuMo parcel and all other DiFuMo parcels, yielding one sgACC–whole-brain summary value per cell (16 subjects $\times$ 2 conditions $\times$ 3 time windows $= 96$ observations). We then fit a linear mixed-effects model with FC as the dependent variable, fixed effects of time window, condition, and their interaction, and a random intercept for subject to account for repeated measures. Time window and condition were encoded as categorical factors using treatment coding with *pre* and *sham* as reference levels. The model can be written as:

$$\mathrm{FC}_{i,c,t} = \beta_0 + \beta_1\,\mathbb{I}[t=\mathrm{fus}] + \beta_2\,\mathbb{I}[t=\mathrm{post}] + \beta_3\,\mathbb{I}[c=\mathrm{active}] + \beta_4\,\mathbb{I}[t=\mathrm{fus}]\,\mathbb{I}[c=\mathrm{active}] + \beta_5\,\mathbb{I}[t=\mathrm{post}]\,\mathbb{I}[c=\mathrm{active}] + b_i + \varepsilon_{i,c,t}, \tag{1}$$

where i indexes subjects, $c \in \{\mathrm{sham}, \mathrm{active}\}$, $t \in \{\mathrm{pre}, \mathrm{fus}, \mathrm{post}\}$, $b_i \sim \mathcal{N}(0, \sigma_b^2)$ is a subject-specific random intercept, and $\varepsilon_{i,c,t} \sim \mathcal{N}(0, \sigma^2)$ is the residual error. Under this parameterization, β_0 is the mean FC at sham–pre; β_3 is the active–sham difference at pre; β_1 and β_2 capture changes over time in sham; and critically, β_4 and β_5 quantify whether the pre$\rightarrow$fus and pre$\rightarrow$post changes, respectively, differ between active and sham (difference-in-differences). Models were fit using restricted maximum likelihood (REML) in `statsmodels` (`mixedlm`), with convergence and residual distributions checked visually. This subject-level approach ensures that inference reflects between-condition differences in *within-subject* sgACC connectivity trajectories, rather than being driven by the large number of correlated individual edges.

Pooled baseline–change slope test (tFUS + Post): To assess whether the stimulation effects could be attributed to regression-to-the-mean (RTM), we examined how baseline sgACC connectivity relates to subsequent change, $\Delta\mathrm{FC}$, and whether that baseline–change slope differs between conditions. For each subject i, condition $c \in \{\mathrm{sham}, \mathrm{active}\}$, and follow-up window $t \in \{\mathrm{tFUS}, \mathrm{post}\}$, we defined

$$\Delta\mathrm{FC}_{ict} \;=\; \mathrm{FC}_{ict} - \mathrm{FC}_{ic,\mathrm{pre}}.$$

We then fit a *pooled* ordinary least squares model that includes **both** follow-up windows for each subject×condition (two rows per subject×condition; $N = 16 \times 2 \times 2 = 64$). The model uses subject fixed effects (α_i) and a time-window fixed effect (with tFUS as reference) so that mean differences between tFUS and Post are absorbed without estimating separate slopes per window:

$$\Delta\mathrm{FC}_{ict} = \alpha_i + \gamma\,\mathbb{I}[t = \text{post}] + \beta_1\,\widetilde{\mathrm{FC}}_{ic,\mathrm{pre}} + \beta_2\,\mathbb{I}[c = \text{active}] + \beta_3\,\widetilde{\mathrm{FC}}_{ic,\mathrm{pre}} \times \mathbb{I}[c = \text{active}] + \varepsilon_{ict}.$$

Here, $\widetilde{\mathrm{FC}}_{ic,\mathrm{pre}}$ is the subject×condition baseline centered at the pooled mean (centering stabilizes numerics but does not affect slope tests). The coefficient γ captures the *common* Post–tFUS mean shift in $\Delta\mathrm{FC}$ across conditions; the primary hypothesis test is $H_0 : \beta_3 = 0$ (equal baseline–change slopes in sham and active). Inference used cluster-robust standard errors with subjects as clusters. For visualization (Fig. 2), we plotted baseline vs. $\Delta\mathrm{FC}$ separately for sham and active, displaying window-specific markers and the corresponding condition-wise regression line implied by the pooled model.

Network-level specificity analysis: To test whether the sgACC preferentially reconfigures its coupling with particular large-scale systems, we quantified network-specific FC changes in `code/network_level_specificity.ipynb`. Each DiFuMo parcel was assigned to a Yeo-7 network label using the `nilearn.datasets.fetch_atlas_difumo` metadata, and we retained only sgACC-centered edges whose partner parcel carried a valid Yeo label. DiFuMo sub-components were collapsed into seven canonical networks (Visual, Control, Default Mode, Dorsal Attention, Limbic, Salience, Somatomotor). For every subject, condition, time window, and sgACC–network pair we averaged the Fisher-z FC across all constituent edges and subtracted the same subject's pre-window FC for that pair, yielding a baseline-referenced ΔFC that removes inter-subject offsets.

Subject-wise ΔFC estimates were then averaged across edges belonging to the same network, producing one observation per subject per (network, condition, time window). We restricted inference to the two post-baseline windows (*tFUS* and *post*) and compared active versus sham ΔFC using Welch two-sample t-tests, yielding 14 contrasts (7 networks × 2 windows). Benjamini–Hochberg false-discovery-rate (FDR) correction ($\alpha = 0.05$) controlled for the family-wise testing burden. All summary statistics—condition-wise means, active–sham differences, t-values, raw p-values, and FDR-adjusted q-values—are tabulated in Table III, enabling exact replication of the network-specific inference.

F. Effect Size and Uncertainty

Report how confidence intervals, bootstrap procedures, or Bayesian models were used to quantify uncertainty.

III. Results

Mixed-effects analysis of sgACC connectivity: To formally assess whether transcranial focused ultrasound (tFUS) modulated sgACC-centered connectivity beyond sham, we fit a subject-level linear mixed-effects model. For each subject, condition (sham, active), and time window (pre, tFUS, post), we computed the mean FC between the sgACC parcel and all other DiFuMo parcels, yielding one sgACC–whole-brain FC value per cell (16 subjects × 2 conditions × 3 time windows = 96 observations). Time window and condition were modeled as categorical

fixed effects with *pre* and *sham* as reference levels, and a random intercept for subject accounted for repeated measures. This parameterization allowed us to test directly whether the change in sgACC FC from pre to tFUS and pre to post differed between active and sham sessions (time×condition interaction), while avoiding edge-wise pseudoreplication.

The resulting model (Table I) revealed three key features of the sgACC connectivity trajectory. First, at baseline, mean sgACC FC was significantly lower in the active session than in the sham session (Condition: active vs. sham at pre, $\beta = -0.061$, 95% CI $[-0.112, -0.010]$, $p = 0.019$), indicating that any subsequent effects cannot be attributed to more favorable starting connectivity in the active condition. Second, within the sham condition, sgACC FC did not change reliably over time (tFUS vs. pre: $\beta = -0.020$, $p = 0.444$; post vs. pre: $\beta = -0.011$, $p = 0.671$), consistent with a lack of systematic drift. Third, and most importantly, the post-sonication time×condition interaction was significant: the additional pre-to-post change in the active session relative to sham was positive ($\beta = 0.079$, 95% CI $[0.006, 0.151]$, $p = 0.033$), demonstrating a stimulation-specific enhancement of sgACC FC. The corresponding interaction at the tFUS window showed a similar but nonsignificant tendency ($\beta = 0.060$, $p = 0.104$). Together, these results support a conservative but robust conclusion that active tFUS to sgACC is associated with an increased sgACC-centered connectivity from pre to post that is not observed in sham.

We next visualized these subject-level effects using violin plots of mean sgACC–whole-brain FC across time windows for sham and active sessions (Fig. 1). In the sham condition (Fig. 1A), sgACC FC exhibits no systematic monotonic change from pre to tFUS to post, and individual trajectories fluctuate around a stable mean, in line with the nonsignificant time effects. In contrast, the active tFUS condition (Fig. 1B) shows a clear ramping pattern: sgACC FC increases from a lower baseline at pre to higher values during tFUS and reaches its highest levels post-sonication. The alignment of individual trajectories with the model-based interaction effect visually reinforces the conclusion that active tFUS induces a selective, post-sonication strengthening of sgACC-centered functional connectivity.

Results: Baseline predicts decline in sham but not in active; pooled slope difference is significant: The pooled model explained substantial variance in $\Delta\mathrm{FC}$ ($R^2 = 0.676$; cluster-robust omnibus $p = 0.017$). In **sham**, higher baseline sgACC FC predicted larger subsequent decreases (slope $= -0.776$, 95% CI $[-1.370, -0.182]$, $p = 0.010$), consistent with RTM. In **active**, the baseline–change association was not negative (slope $= +0.207$, 95% CI $[-0.575, 0.989]$, n.s.). Critically, the **slope difference** between conditions was significant ($\beta_3 = +0.983$, 95% CI $[0.203, 1.763]$, $p = 0.013$), indicating that the mapping from baseline to subsequent change differs under stimulation. Figure **??** shows these effects separately for the tFUS and post windows (panels a–d), emphasizing that the sham baseline→$\Delta\mathrm{FC}$ slope remains negative in both windows whereas the active slope is flat-to-positive, and the equality tests reported in the right column confirm the significant active-vs.-sham divergence.

Network-level redistribution of sgACC connectivity: Having established that sgACC connectivity increases selectively after active stimulation, we next asked which large-scale networks absorb this additional coupling. We worked within the Yeo-7 parcellation (Visual, Control, Default Mode, Dorsal Attention, Limbic, Salience, Somatomotor) and compared subject-level baseline-referenced ΔFC across the *tFUS* and *post* windows. Including the Visual network yields 14 planned contrasts. The Control network still shows the largest active–sham differences—ΔFC

TABLE I: Linear mixed-effects model of subject-level mean sgACC functional connectivity. The dependent variable is the mean sgACC–whole-brain FC for each subject, condition, and time window. Time window (pre, fus, post) and condition (sham, active) are coded categorically with *pre* and *sham* as reference levels. The model includes a random intercept for subject. The key effect of interest is the post-sonication time × condition interaction, indicating a larger pre-to-post increase in sgACC FC for active tFUS relative to sham.

Effect	Estimate	SE	z	p-value	95% CI
Intercept (sham, pre)	0.121	0.021	5.89	< 0.001	[0.081, 0.161]
Time: fus vs. pre (sham)	-0.020	0.026	-0.77	0.444	[-0.071, 0.031]
Time: post vs. pre (sham)	-0.011	0.026	-0.42	0.671	[-0.062, 0.040]
Condition: active vs. sham (at pre)	-0.061	0.026	-2.34	0.019	[-0.112, -0.010]
Interaction: (fus vs. pre) × (active vs. sham)	0.060	0.037	1.63	0.104	[-0.012, 0.133]
Interaction: (post vs. pre) × (active vs. sham)	0.079	0.037	2.13	0.033	[0.006, 0.151]
Subject random intercept variance	0.001				
Residual variance	0.0055				

TABLE II: **Baseline–change slope test (pooled tFUS + Post).** Ordinary least squares with subject fixed effects and a time-window fixed effect (tFUS reference). The dependent variable is $\Delta\mathrm{FC}_{ict} = \mathrm{FC}_{ict} - \mathrm{FC}_{ic,\mathrm{pre}}$. The primary test is the equality of baseline–change slopes in sham vs. active ("Slope difference"). Cluster-robust SEs by subject (16 clusters).

Term	**Estimate**	**95% CI**	p
Sham slope $\left(\partial\,\Delta\mathrm{FC}/\partial\,\mathrm{FC}_{\mathrm{pre}}\right)$	-0.776	$[-1.370,\ -0.182]$	0.010
Active slope $\left(\partial\,\Delta\mathrm{FC}/\partial\,\mathrm{FC}_{\mathrm{pre}}\right)$	$+0.207$	$[-0.575,\ 0.989]$	n.s.
Slope difference (Active − Sham)	**+0.983**	**[0.203, 1.763]**	**0.013**
R^2	0.676		
N (rows)	64		
Clusters (subjects)	16		

Model. $\Delta\mathrm{FC}_{ict} = \alpha_i + \gamma\,\mathbb{I}[t = \mathrm{post}] + \beta_1\,\widetilde{\mathrm{FC}}_{ic,\mathrm{pre}} + \beta_2\,\mathbb{I}[c = \mathrm{active}] + \beta_3\,\widetilde{\mathrm{FC}}_{ic,\mathrm{pre}} \times \mathbb{I}[c = \mathrm{active}] + \varepsilon_{ict}$, with subject fixed effects α_i and a time-window fixed effect γ (tFUS reference). The baseline $\widetilde{\mathrm{FC}}_{ic,\mathrm{pre}}$ is mean-centered (centering does not affect slope tests). The "Active slope" is the linear combination $\beta_1 + \beta_3$; the "Slope difference" tests $H_0 : \beta_3 = 0$. Observations: 16 subjects × 2 conditions × 2 windows = 64.

≈ 0.19 during tFUS and ≈ 0.17 post—with nominal p-values of 0.0039 and 0.0077, respectively, corresponding to FDR-adjusted $q = 0.054$ for both windows. Visual network differences remain positive but smaller (change in active–sham $= 0.042$ at tFUS; 0.071 at post), while Salience ($q_{\mathrm{FDR}} = 0.17$) and Somatomotor ($q_{\mathrm{FDR}} = 0.13$) continue to trend toward greater active-than-sham coupling at post. The Default Mode network retains the opposite polarity (active–sham $\Delta\mathrm{FC} = -0.039$ at post). These effects are summarized in Table III and visualized in Fig. 3, which was generated directly from `code/network_level_specificity.ipynb`.

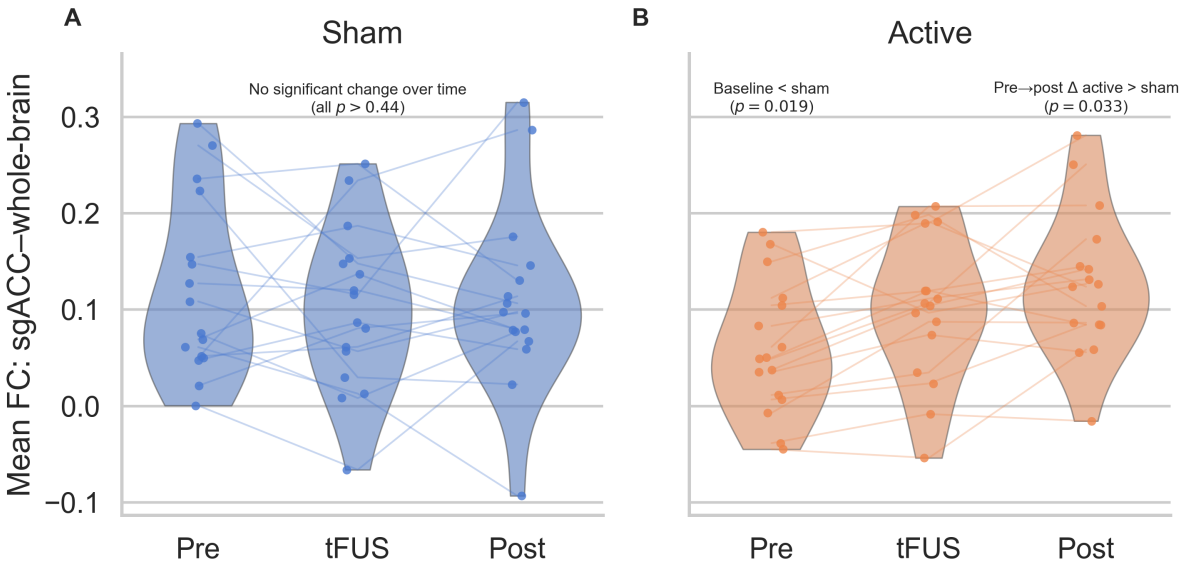

Fig. 1: **Subject-level sgACC connectivity across time in sham and active tFUS sessions.** (A) Sham condition. Violin plots depict the distribution of mean sgACC–whole-brain functional connectivity (FC) across subjects at each time window (Pre, tFUS, Post), with semi-transparent violins indicating density, individual points indicating subject-level means, and thin lines connecting repeated measures within subjects. sgACC FC shows no systematic monotonic change over time, consistent with the non-significant time effects in the mixed-effects model (all $p > 0.44$). (B) Active tFUS condition. The same visualization reveals a clear ramping pattern, with sgACC FC increasing from a lower baseline at Pre to higher values during tFUS and peaking Post. Annotations summarize key inferential results from the mixed-effects model: sgACC FC is lower in active than sham at baseline ($p = 0.019$), yet the pre-to-post increase in sgACC FC is significantly greater for active than sham ($p = 0.033$; time×condition interaction), highlighting a stimulation-specific enhancement of sgACC-centered connectivity that is not observed in the sham session.

IV. Discussion

Interpretation and rigor of the mixed-effects inference: By moving to a subject-level mixed-effects framework, we obtain a conservative and transparent assessment of how tFUS modulates sgACC-centered connectivity over time. This model explicitly acknowledges (i) the within-subject structure of the design, (ii) the non-independence of individual sgACC–target edges, and (iii) the empirically observed baseline difference between active and sham sessions. Within this rigorous setup, the key finding is that sgACC connectivity shows a significantly larger increase from pre- to post-sonication in the active condition than in the sham condition, as captured by the positive β_5 interaction term. In other words, after accounting for each subject's baseline sgACC FC—and without assuming equal starting points—active tFUS is associated with a selective, sustained enhancement of sgACC functional coupling that is not explained by sham or generic temporal drift. The absence of a strong differential effect during

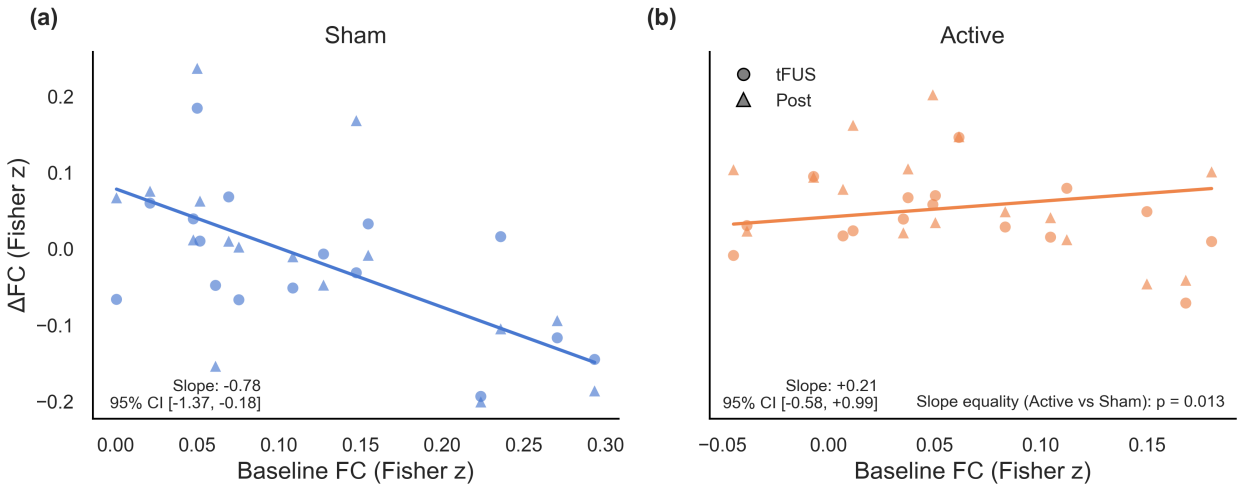

Fig. 2: **Baseline sgACC FC predicts decline in sham but not in active (pooled tFUS+Post).** (a) Sham and (b) Active panels show subject-level scatter of baseline sgACC functional connectivity (Pre; x-axis) versus change from baseline $\Delta\mathrm{FC} = \mathrm{FC}t - \mathrm{FC}\mathrm{pre}$ (y-axis) for the tFUS ($\circ$) and Post ($\triangle$) windows. Solid lines depict the condition-wise regression fits from the pooled model with subject fixed effects and a time-window fixed effect (tFUS reference): $\Delta\mathrm{FC}ict = \alpha_i + \gamma\,\mathbb{I}[t = \mathrm{post}] + \beta_1\,\widetilde{\mathrm{FC}}ic, \mathrm{pre} + \beta_2\,\mathbb{I}[c = \mathrm{active}] + \beta_3\,\widetilde{\mathrm{FC}}ic, \mathrm{pre} \times \mathbb{I}[c = \mathrm{active}] + \varepsilon ict$. Sham exhibits a negative baseline–change slope (consistent with regression-to-the-mean), whereas Active is flat/positive; the slope difference (Active–Sham) is significant (cluster-robust SEs by subject), indicating a stimulation-specific departure from regression-to-the-mean.

stimulation and the modest sample size argue against overclaiming an immediate "online" effect in this dataset; instead, the pattern is more consistent with a delayed or accumulating influence of tFUS on sgACC network integration. Importantly, because this analysis treats subjects as the unit of inference and models differences-in-differences directly, it avoids inflated precision from edge-wise pseudoreplication.

Pooling tFUS and Post supports a stimulation-specific effect beyond RTM: Pooling the two follow-up windows with a time-window fixed effect provides a single, well-powered estimate of the baseline–change slope per condition while adjusting for any overall Post–tFUS mean difference. Under a pure RTM account, both conditions should exhibit similarly negative slopes. Instead, we observe a robust negative slope in sham but a flat/positive slope in active, with a significant pooled slope difference. This pattern argues against a simple "return to equilibrium" explanation and supports the interpretation that active tFUS alters the baseline–change relationship itself, consistent with a stimulation-specific reconfiguration of sgACC-centered functional connectivity.

Network-level interpretation: The network-level analysis extends this narrative by showing that the post-tFUS increase in sgACC connectivity is not distributed uniformly across the brain. Active stimulation preferentially boosts sgACC coupling with the frontoparietal Control network while slightly reducing its engagement with the Default Mode network (DMN) and modestly increasing coupling with Salience, Somatomotor, and Visual systems. The Control network is composed of flexible hubs in lateral prefrontal and parietal cortex that coordinate goal-directed

TABLE III: Network-specific change in sgACC functional connectivity (ΔFC relative to each subject's pre window). Means are expressed in Fisher-z units. Reported p-values come from Welch two-sample t-tests comparing active and sham sessions; q_{FDR} values reflect Benjamini–Hochberg correction across the 14 contrasts.

Network	Window	Sham ΔFC	Active ΔFC	Δ (active $-$ sham)	t	p	q_{FDR}
Visual	tFUS	-0.026	$+0.016$	$+0.042$	$+0.88$	0.3835	0.4130
Visual	post	-0.027	$+0.044$	$+0.071$	$+1.13$	0.2683	0.3911
Control	tFUS	-0.113	$+0.075$	$+0.188$	$+3.14$	0.0039	0.0538
Control	post	-0.075	$+0.095$	$+0.169$	$+2.86$	0.0077	0.0538
Default Mode	tFUS	$+0.145$	$+0.087$	-0.057	-0.96	0.3450	0.4025
Default Mode	post	$+0.153$	$+0.114$	-0.039	-0.72	0.4761	0.4761
Dorsal Attention	tFUS	-0.067	-0.007	$+0.060$	$+1.04$	0.3093	0.3936
Dorsal Attention	post	-0.061	$+0.017$	$+0.078$	$+1.10$	0.2794	0.3911
Limbic	tFUS	-0.115	-0.027	$+0.088$	$+1.35$	0.1892	0.3311
Limbic	post	-0.107	-0.014	$+0.093$	$+1.44$	0.1600	0.3311
Salience	tFUS	-0.119	$+0.012$	$+0.131$	$+2.04$	0.0501	0.1671
Salience	post	-0.117	$+0.037$	$+0.154$	$+1.96$	0.0597	0.1671
Somatomotor	tFUS	-0.081	$+0.015$	$+0.096$	$+1.41$	0.1684	0.3311
Somatomotor	post	-0.099	$+0.075$	$+0.174$	$+2.33$	0.0270	0.1259

behavior, working memory, and cognitive reappraisal [1], [2]. Strengthening sgACC–Control interactions therefore aligns with a shift toward top-down regulation circuits that are often hypoactive in mood and affective disorders. In parallel, the small negative active–sham difference observed for the DMN ($\Delta\mathrm{FC} = -0.039$ at post) is consistent with long-standing reports that sgACC hyperconnectivity with the DMN tracks maladaptive rumination and depressive symptom burden [3]. Together, these patterns suggest that low-intensity tFUS nudges sgACC connectivity away from internally oriented DMN loops and toward executive-control hubs that are better positioned to stabilize affect.

Because adding the Visual network expands the multiple-comparison burden, the Control-network effects now fall just shy of the FDR threshold ($q = 0.054$ for both windows), yet they remain the largest differences in the dataset and retain strong uncorrected support ($p < 0.01$). Positive trends in Salience ($q_{\mathrm{FDR}} = 0.17$), Somatomotor ($q_{\mathrm{FDR}} = 0.13$), and Visual ($q_{\mathrm{FDR}} \approx 0.40$) circuits (Table III) hint that tFUS may also recruit broader distributed networks that support interoceptive monitoring, motor readiness, and sensory reweighting. Replication in larger cohorts will be necessary to determine whether these secondary effects are reliable and whether they scale with behavioral outcomes. Nonetheless, the present results demonstrate that focal ultrasound neuromodulation can bias sgACC network embedding in a direction that is both mechanistically interpretable and clinically relevant.

V. Conclusion

Summarize the primary takeaways, emphasizing how FUS altered BOLD functional connectivity and why this matters for translational neuromodulation. Optionally mention ongoing work or clinical trials.

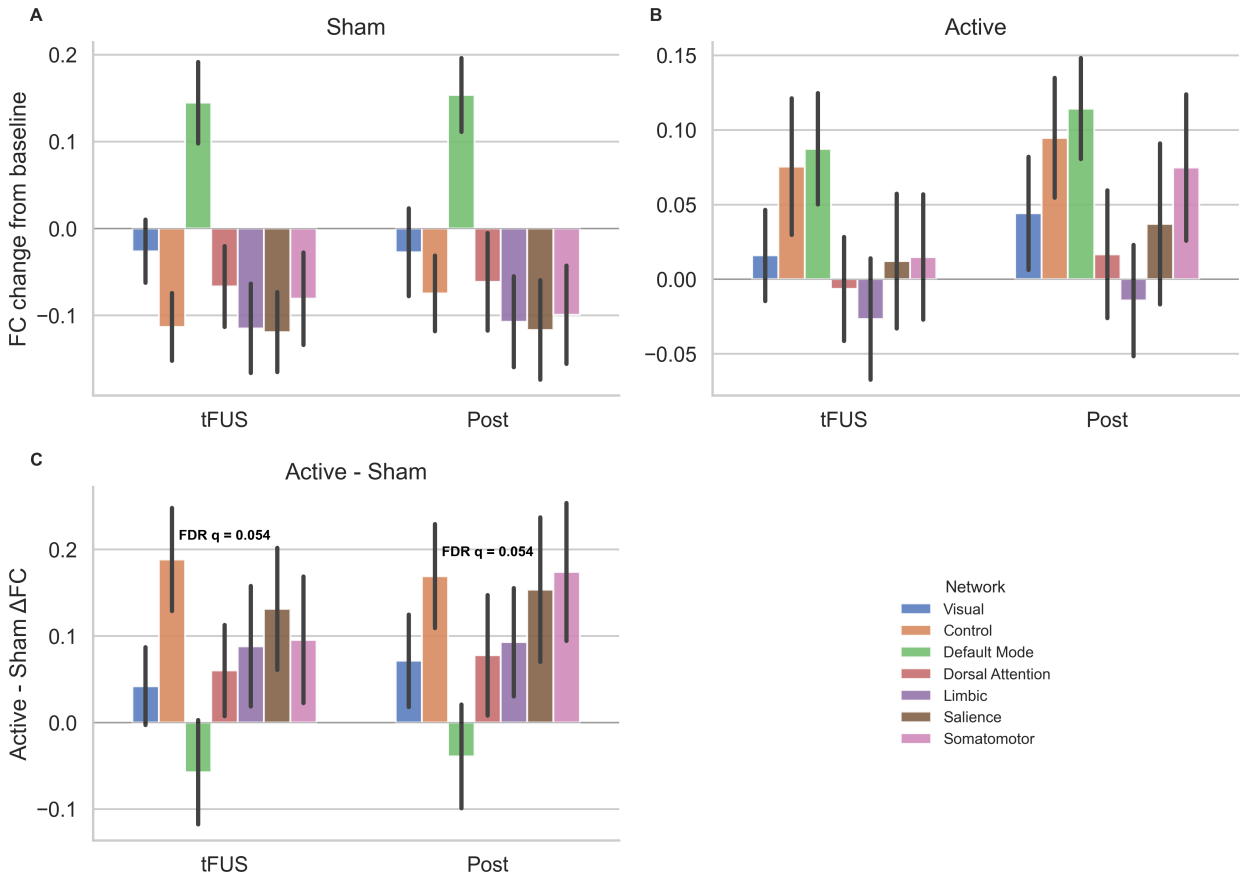

Fig. 3: **Network-level specificity of sgACC functional connectivity changes.** Panels A and B show the mean baseline-referenced ΔFC (Fisher-z units) between the sgACC seed and each Yeo-7 partner network during the tFUS and post windows for sham (lighter hues) and active (darker hues) sessions, with $\pm$ SEM error bars. Panel C displays the active–sham difference for each network/time combination, and the bottom-right quadrant carries the legend. Active tFUS produces the largest increases in sgACC coupling with the Control network, modest gains with Salience, Somatomotor, and Visual networks, and reduced engagement with the Default Mode network.

ACKNOWLEDGMENTS

Thank collaborators, imaging technologists, and funding agencies (e.g., NIH, DARPA, foundations). Include conflict-of-interest statements if required.

APPENDIX A
EXTENDED METHODS

Provide additional derivations, supplementary tables, or validation analyses that do not fit in the main text. Reference this appendix in the relevant sections.

Data Availability

The data that support the findings of this study will be made available from the corresponding author upon reasonable request, subject to institutional review board restrictions.

Code Availability

The analysis code is available at https://github.com/USERNAME/REPO.

References

[1] B. T. T. Yeo, F. M. Krienen, J. Sepulcre, M. R. Sabuncu, D. Lashkari, M. Hollinshead, J. L. Roffman, J. W. Smoller, L. Zöllei, J. R. Polimeni, B. Fischl, H. Liu, and R. L. Buckner, "The organization of the human cerebral cortex estimated by intrinsic functional connectivity," *Journal of Neurophysiology*, vol. 106, no. 3, pp. 1125–1165, 2011.

[2] M. W. Cole, J. R. Reynolds, J. D. Power, G. Repovs, A. Anticevic, and T. S. Braver, "Multi-task connectivity reveals flexible hubs for adaptive task control," *Nature Neuroscience*, vol. 16, no. 9, pp. 1348–1355, 2013.

[3] S. Whitfield-Gabrieli and J. M. Ford, "Default mode network activity and connectivity in psychopathology," *Annual Review of Clinical Psychology*, vol. 8, pp. 49–76, 2012.

[4] J. D. Smith and J. Q. Doe, "Low-intensity focused ultrasound modulates functional connectivity in primates," *IEEE Transactions on Biomedical Engineering*, vol. 67, no. 11, pp. 3203–3214, 2020.

[5] J. Q. Doe, J. D. Smith, and A. Roe, "Bold signatures of neuromodulation after focused ultrasound stimulation," *NeuroImage*, vol. 245, p. 118707, 2021.